Journal of Great Lakes Research 35 (2009) 361–370

Contents lists available at ScienceDirect

Journal of Great Lakes Research

journal homepage: www.elsevier.com/locate/jglr

Assessing the application of SeaWiFS ocean color algorithms to Lake Erie

Donna L. Witter [a,*], Joseph D. Ortiz [a], Sarah Palm [b,1], Robert T. Heath [b], Judith W. Budd [c,2]

[a] Department of Geology, Kent State University, 221 McGilvrey Hall, Kent, OH 44242, USA
[b] Department of Biological Sciences, Kent State University, 256 Cunningham Hall, Kent, OH 44242, USA
[c] Department of Geological and Mining Engineering and Sciences, Michigan Technological University, Houghton, MI 49931, USA

ARTICLE INFO

Article history:
Received 18 September 2008
Accepted 17 March 2009

Communicated by Ram Yerubandi

Index words:
Remote sensing
Ocean color
Chlorophyll a
Satellite observation
Lake Erie

ABSTRACT

The feasibility of satellite-based monitoring of phytoplankton chlorophyll *a* concentrations in Lake Erie is assessed by applying globally calibrated, ocean-derived color algorithms to spatially and temporally collocated measurements of SeaWiFS remote sensing reflectance. Satellite-based chlorophyll *a* retrievals were compared with fluorescence-based measurements of chlorophyll *a* from 68 field samples collected across the lake between 1998 and 2002. Twelve ocean-derived color algorithms, one regional algorithm derived for the Baltic Sea's Case 2 waters, and a set of regional algorithms developed for the western, central and eastern basins of Lake Erie were considered. While none of the ocean-derived algorithms performed adequately, the outlook for the success of regionally calibrated and validated algorithms, with forms similar to the ocean-derived algorithms, is promising over the eastern basin and possibly the central basin of the lake. In the western basin, each of the regional algorithms considered performed poorly, indicating that alternative approaches to algorithm development, or to satellite data screening and analysis procedures will be needed.

Introduction

Many of the environmental challenges faced by Lake Erie and the populations that depend on its resources could be better addressed if conditions within the lake were more consistently monitored throughout the year and across the basin. These challenges include understanding the impacts of eutrophication, monitoring the severity and extent of seasonal hypoxia, assessing the effects of exotic species on lake ecosystems, detecting and preventing toxic algal blooms and tracking chemically contaminated sediments (Beeton, 2001; Ohio Lake Erie Commission, 2004). Field-based monitoring of ecosystem and physical properties within the lake has greatly enhanced understanding of these and other issues, but, for practical reasons, field sampling programs are generally restricted to a small number of observations in space and time. Satellite remote sensing provides an opportunity to conduct longer-term and more consistent monitoring of color-producing agents (CPAs) within the lake, but this approach must be pursued carefully to ensure that inferences based on satellite data provide an accurate depiction of conditions near the surface of the lake. We seek to better understand the degree to which remotely sensed observations of lake color can be used as part of a longer-term strategy for monitoring near-surface algal biomass within Lake Erie at the spatial and temporal scales resolved by these remote sensing observations. We specifically consider the degree to which empirical, ocean-derived algorithms can be used to estimate phytoplankton chlorophyll *a* concentrations in the three sub-basins of the lake.

Lake Erie is an optically complex environment due to the diversity and inhomogeneous distribution of CPAs within the lake. The lake is divided into three basins with the separation between the western and central basins marked by the Lake Erie Islands at approximately 82°49′W, and the separation between the central and eastern basins marked by the Long Point-Erie Ridge located at approximately 80°25′ W (Fig. 1). Stratification regimes vary along the lake, particularly in the summer, when strong stratification has been observed only in the eastern basin (Barbiero and Tuchman, 2001b). These variations in depth and stratification, as well as variations in nutrient loading, resulted in the shallow western basin being the most biologically productive part of the lake prior to the introduction of the zebra mussel *Dresissena polymorpha* (Makarewicz, 1993). Since then, biological productivity has decreased in the western basin and seasonal variations in the relative productivity of the three basins have been observed (Frost and Culver, 2001; Makarewiczl et al., 1999), though near-surface chlorophyll *a* concentrations continue to be highest in the western basin (Ostrom et al., 2005; Smith et al., 2005). Toxic algal blooms, which contribute to variations in CPAs, have been documented most commonly in the western basin of the lake (Budd et

* Corresponding author.
E-mail addresses: dwitter@kent.edu (D.L. Witter), jortiz@kent.edu (J.D. Ortiz), sarah.palm@bayfront.org (S. Palm), rheath@kent.edu (R.T. Heath), Judith.budd@finlandia.edu (J.W. Budd).
[1] Present address: Bayfront Medical Center, Cytology Department, 701 6th Str. S., St. Petersburg, FL 33701, USA.
[2] Present address: Finlandia University, 601 Quincy Street, Hancock, MI 49930, USA.

0380-1330/$ – see front matter © 2009 Elsevier Inc. All rights reserved.
doi:10.1016/j.jglr.2009.03.002

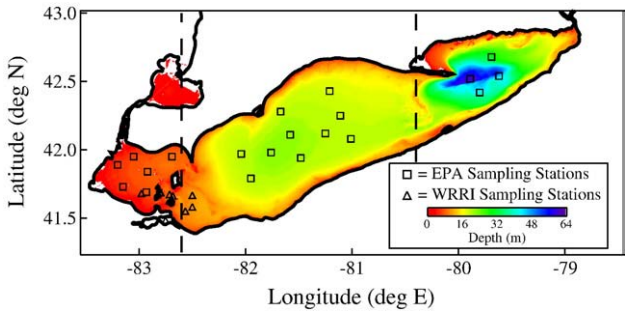

Fig. 1. Locations of field stations used in this analysis (symbols). Note that not all locations are sampled in each year. EPA data (squares) from 1998 to 2002 and WRRI data (triangles) from 1998 and 2002 were used in this analysis. Dashed lines delineate the boundaries used in this study for the western, central and eastern basins of the lake, with bathymetry shown using shading. Bathymetry provided by the National Geophysical Data Center (1998).

al., 2001; Vincent et al., 2004), and are expected to become more wide-spread in the future (Conroy et al., 2007). In addition to these variations in biological properties, most of the major rivers draining into Lake Erie empty into the western basin, where they deposit much of their accumulated sediment load (Kemp et al., 1977). This flux, and the resuspension of bottom sediments (Dusini et al., 2009; Marvin et al., 2007), contribute to the higher levels of turbidity observed in the shallow western basin as compared with other basins of the lake (Markarewiczl et al., 1999). Suspended sediments are a particular concern as they can be carriers of chemical contaminants (Marvin et al., 2002, 2004, 2007; Painter et al., 2001).

As a result of variations in the loading of suspended sediments and biological materials within the euphotic zone, Lake Erie represents a significant challenge to the interpretation of satellite-based water color observations. Ocean color sensors have however been successfully used in North American Great Lakes. For example, Shuchman et al. (2006) derived a 7-year time series of chlorophyll *a* for Lake Michigan using observations from the Sea-viewing Wide Field-of-view Sensor (SeaWiFS). Kerfoot et al. (2008) used both SeaWiFS and the MOderate-Resolution Imaging Spectroradiometer (MODIS) to detect intra-seasonal variations in near-surface chlorophyll *a* in southern Lake Michigan. Budd (2004) used SeaWiFS to track the biological signal of a sediment plume in the Keweena Region of Lake Superior. Binding et al. (2007) used Coastal Zone Color Scanner observations spanning the period 1979–1985 and SeaWiFS observations spanning the period 1998–2006 to monitor changes in the clarity of the lower Great Lakes. This analysis revealed significant changes in the clarity of Lakes Erie and Ontario associated with the long-term impact of the zebra mussel invasion.

In ocean settings, estimates of chlorophyll *a* concentration are obtained by applying empirical or semi-analytic algorithms to water properties measured by satellite-mounted visible and infrared sensors. The most straightforward application of ocean color algorithms to the problem of estimating biological productivity occurs in Case 1 waters, where optical properties are dominated by phytoplankton and their covarying degradation products (Morel and Prieur, 1977). Case 2 waters represent more complex optical settings, which may include phytoplankton, suspended sediments and other water-borne materials (see Mobley et al. (2004) and Morel and Prieur (1977)). Within the relatively confined setting of Lake Erie, biological and sedimentological conditions can vary significantly (Kemp et al., 1977; Makarewicz, 1993; Marvin et al., 2007), resulting in potentially diverse optical conditions. While some regions of the lake may satisfy conditions for Case 1 waters, other regions may represent an extreme end member of Case 2 waters.

In this study we explore the feasibility of monitoring near-surface phytoplankton chlorophyll *a* concentrations in the three basins of Lake Erie using observations from the SeaWiFS satellite ocean color sensor. Values of chlorophyll *a* concentration measured from samples collected in the field are compared with estimates computed by applying ocean-derived color algorithms to spatially and temporally collocated measurements of remote sensing reflectance from SeaWiFS. The next sections of this paper describe the field-collected and satellite datasets and the methodology used in this study. Then results from the analysis, including a statistically based interpretation of differences between the field-collected and satellite results are presented. Lastly, we discuss prospects for long-term monitoring of phytoplankton in Lake Erie using ocean color satellite sensors.

Data

Field samples

The approach in this study is based on statistical comparisons of spatially and temporally collocated chlorophyll *a* concentrations measured from field samples and estimated from remote sensing reflectances observed by the SeaWiFS satellite ocean color sensor. Chlorophyll *a* concentrations were measured from bottle samples collected in the field by the U.S. Environmental Protection Agency (EPA) and made available through the Great Lakes Environmental Database. The EPA data used in this study were collected on cruises that occurred during spring (March or April) and summer (August) of each year from 1998 through 2002. Additional samples were collected by Kent State University's Water Resources Research Institute (WRRI) during a separate series of five cruises within the western and central basins of the lake during June, July and August of 1998 and during July and August of 2002. The chlorophyll *a* concentrations in both sets of bottle samples were measured based on chlorophyll fluorescence. Data collection procedures used by the EPA are described by Barbiero and Tuchman (2001a). Samples collected by Kent State University were analyzed using the US EPA Fluorometric method 445.0 (Arar and Collins, 1997).

Sampling stations were distributed throughout the three basins of the lake (Fig. 1), with highest station density in the western basin. Each data record consists of the measured value of chlorophyll *a* concentration, the depth from which the sample was collected, the time and date of collection, and the latitude and longitude of the sample location. Secchi depth was reported for 46% of casts, and 95% of casts included samples collected from three or more depths. While this dataset is relatively comprehensive in terms of spatial coverage of the lake and the number of years sampled during the SeaWiFS period, these data were collected for the purpose of field-based biological sampling, rather than a full bio-optical evaluation. Thus observations of optical properties of the water column, such as the diffuse attenuation coefficient (K_d), the concentration of chromophoric dissolved organic material (CDOM), and the upwelling and downwelling irradiance (E_u and E_d), are not available.

The field-collected dataset was screened to eliminate observations with chlorophyll *a* concentrations greater than 20 μg/L and observations where the shallowest sample depth was greater than 10 m. This eliminated two observations from the highly eutrophic and turbid Sandusky Bay (latitude = 41.48°N, longitude = 82.75°W), where the chlorophyll *a* concentration was measured as 66.0 and 81.1 μg/L, and where chlorophyll *a* concentrations are known from prior work to exceed 20 μg/L (Ostrom et al., 2005). This also eliminated one observation from the central basin in which the depth of the shallowest sample was recorded as 43.8 m, which is deeper than the maximum depth of this basin. The data were then screened to eliminate observations within 2 km of land to reduce the possible impact of land contamination within the satellite footprint. Potential outliers, which had relatively high chlorophyll *a*, were then carefully examined. Each of these was found to be consistent with elevated chlorophyll *a* measured at other stations in the same basin on the same cruise or measured at slightly deeper depths at the same station

and time. These observations were thus retained in the collocated dataset. After applying all of these screening procedures, the field-collected dataset contained observations from 224 casts, including 69 in the western basin, 112 in the central basin and 43 in the eastern basin.

SeaWiFS observations

Remotely sensed observations of lake color were obtained using the SeaWiFS optical scanner. The SeaWiFS datasets used in this study were processed at Michigan Technological University (MTU) from SeaWiFS level 1A data using the SeaWiFSMAP 4.1a software package (Stumpf et al., 2000). SeaWiFSMAP was developed by modifying the commonly used SEADAS software package to better suit optical conditions of coastal and inland waters. Unlike SEADAS, SeaWiFSMAP uses a USGS map for georectification. The Stumpf et al. (2003) atmospheric correction algorithm, derived for inland water bodies, including the Great Lakes, was applied to the data in SeaWiFSMAP (see Budd (2004) and Budd and Warrington (2004)). Values of remote sensing reflectance (R_{rs}) at 443 nm, 490 nm, 512 nm, and 555 nm were downloaded from the MTU Great Lakes Imagery Archive and converted to estimates of chlorophyll concentration using twelve previously published empirical ocean color algorithms (Table 1). For algorithms that used normalized water-leaving radiance (L_{wn}) as input, R_{rs} values were converted to L_{wn} using values of mean solar irradiance (F_0) at each wavelength (Thuillier et al., 2003).

Methodology

To assess the degree to which twelve ocean-derived satellite chlorophyll concentration algorithms accurately estimate Lake Erie chlorophyll *a* concentrations, chlorophyll *a* concentrations measured from samples collected in the field were compared with collocated SeaWiFS-derived estimates. For each field observation, SeaWiFS R_{rs} values that were measured within 1 day of field sampling were extracted from the pixel that coincided with the field-based sampling location. To reduce the impacts of atmospheric contamination, screening procedures similar to those used by Budd and Warrington (2004) were then applied. The percentage of masked pixels over the lake was calculated for each satellite image and cases where lake-wide masking exceeded 20% of the total lake pixels were deleted. Field-satellite observation pairs that were located within 5 km of the nearest masked pixel were also eliminated. As there is no general consensus regarding the criteria for cloud, haze and aerosol masking for the Great Lakes, choices of the lake-wide percent masking criterion and the threshold for proximity to the nearest masked pixel are somewhat arbitrary. Alternative values were considered and are discussed below.

Most of the field casts included samples collected at several depths. A number of methods for including depth-dependent information were considered, including averaging data over the upper part of the water column and integrating the chlorophyll *a* measurements down to various percentages of the Secchi depth. Because the vertical sampling varied within the dataset, with some casts having relatively high vertical resolution and others having coarser vertical resolution, and because many records lacked observations of the Secchi depth, none of these alternative methods provided statistical comparisons which improved on those available by using only the uppermost sample from each cast. Thus this analysis uses only the uppermost chlorophyll *a* concentration measurement from each cast.

The resulting spatially and temporally collocated dataset included 68 field-satellite observation pairs at 20 unique station locations that were sampled on 9 separate cruises. Of these, 18 were in the western basin (6 station locations, 6 cruises), 30 were in the central basin (10 station locations, 5 cruises), and 20 were in the eastern basin (4 station locations, 6 cruises). Statistics of the full field-collected and of the collocated datasets are summarized in Table 2. In both datasets, the mean and standard deviation of the chlorophyll *a* concentrations decreased from west to east, in agreement with trends observed in previous studies of chlorophyll *a* (Makarewiczl et al., 1999; Ostrom et al., 2005; Smith et al., 2005).

Table 1
Algorithms used to estimate chlorophyll *a* concentration (C) or chlorophyll *a* + phaeophytic concentration [$C+P$] in μg/L from observations of remote sensing reflectance (R_{rsnnn}) or normalized water-leaving radiance (L_{wnnnn}) at wavelengths *nnn* nm.

Algorithm	Algorithm equation	Reference
Morel-1	$C = 10\text{^}(0.2492 - 1.768R)$ $R = \log(R_{rs443}/R_{rs555})$	O'Reilly et al. (1998)
Morel-3	$C = 10\text{^}(0.20766 - 1.82878R + 0.75885R^2 - 0.73979R^3)$ $R = \log(R_{rs443}/R_{rs555})$	O'Reilly et al. (1998)
Coastal	$C_{se} = 10\text{^}(-2.5R)$, where $R = \log(R_{rs490}/R_{rs555})$ If $C_{se} \geq 0.5$ then $C = C_{se}$ If $0.1 < C_{se} < 0.5$ then $C = 10\text{^}(\log(C_{se}) * [\log(C_{se}) - \log(0.1)]/[\log(0.5)\ \log(0.1)]$ $+ \log(C_{Oc2v4}) * [\log(0.5) - \log(C_{se})]/[\log(0.5) - \log(0.1)]$ If $C_{se} \leq 0.1$ then $C = C_{Oc2v4}$	Stumpf et al. (2000)
Aiken-P	$C_{22} = \exp(0.696 - 2.085\ \ln(R))$ $C_{24} = (R - 5.29)/(0.592 - 3.48R)$ where $R = L_{wn490}/L_{wn555}$ $[C+P] = C_{22}$; if $[C+P] < 2.0$ μg/L then $[C+P] = C_{24}$	Aiken et al. (1995)
Aiken-C	$C_{21} = \exp(0.464 - 1.989\ \ln(R))$ $C_{23} = (R - 5.29)/(0.719 - 4.23R)$ where $R = L_{wn490}/L_{wn555}$ $C = C_{21}$; if $C < 2.0$ μg/L then $C = C_{23}$	Aiken et al. (1995)
CalCOFI two-band linear	$C = 10\text{^}(0.444 - 2.431R)$ where $R = \log(R_{rs490}/R_{rs555})$	Michell and Kahru (1998)
Morel-2	$C = \exp(1.077835 - 2.542605R)$ $R = \ln(R_{rs490}/R_{rs555})$	O'Reilly et al. (1998)
CalCOFI three-band	$C = \exp(1.025 - 1.622R_1 - 1.238R_2)$ $R_1 = \ln(R_{rs490}/R_{rs555})$ $R_2 = \ln(R_{rs510}/R_{rs555})$	Michell and Kahru (1998)
Oc2v4	$C = 10\text{^}(0.319 - 2.336R + 0.879R^2 - 0.135R^3) - 0.071$ $R = \log(R_{rs490}/R_{rs555})$	O'Reilly et al. (2000)
Morel-4	$C = 10\text{^}(1.03117 - 2.40134R + 0.3219897R^2 - 0.291066R^3)$ $R = \log(R_{rs490}/R_{rs555})$	O'Reilly et al. (1998)
CalCOFI two-band cubic	$C = 10\text{^}(0.450 - 2.860R + 0.996R^2 - 0.367R^3)$ where $R = \log(R_{rs490}/R_{rs555})$	Michell and Kahru (1998)
Oc4v4	$C = 10\text{^}(0.366 - 3.067R + 1.930R^2 + 0.649R^3 - 1.532R^4)$ $R = \log(\max[R_{rs443}, R_{rs490}, R_{rs510}]/R_{rs555})$	O'Reilly et al. (2000)
Baltic	$C = 10\text{^}(0.1520 - 3.0558R)$ where $R = \log(\max[L_{wn443}/L_{wn551}, L_{wn488}/L_{wn551}])$	Darecki and Stramski (2004)

Note that where the maximum operator (max) appears, the largest of the quantities in the square brackets is used.

Table 2
Statistics of the field observations used in this analysis.

Region	Number of observations	z_{top} (average depth of shallowest field-collected sample, m)	Standard deviation of z_{top} (m)	Average chlorophyll *a* concentration of shallowest field-collected sample [μg/L]	Standard deviation of chlorophyll *a* concentration from the shallowest field-collected samples [μg/L]
Western Basin	69 (18)	1.1 (1.2)	0.3 (0.3)	3.7 (3.8)	2.7 (3.0)
Central Basin	112 (30)	1.3 (1.2)	0.7 (0.3)	2.2 (2.1)	1.8 (1.8)
Eastern Basin	43 (20)	1.3 (1.2)	0.5 (0.3)	1.4 (1.4)	1.4 (1.2)
Whole Lake	224 (68)	1.2 (1.2)	0.5 (0.3)	2.5 (2.3)	2.2 (2.2)

Values in parentheses show statistics of observations from the subset of field observations which could be collocated with a satellite observation with a search window of ±1 day while meeting the screening criteria described in the Methodology section.

F-tests for the equality of variance (see Davis, 2002) were applied to the field-collected chlorophyll *a* data from each basin of the lake to assess whether the differences in the distribution of measured values were statistically different between the full dataset and the smaller collocated dataset. Results indicated that the chlorophyll *a* variances were not statistically different at $\alpha = 0.05$, allowing a comparison of the equality of the mean chlorophyll *a* concentrations from the two datasets in each basin of the lake. Results from *t*-tests of the equality of sample means (see Davis, 2002) demonstrated that the mean chlorophyll *a* concentrations were not statistically different at $\alpha = 0.05$ for the full dataset versus the collocated data. These comparisons indicate that, while the collocated dataset is relatively small, it is representative of more extensive variations within each basin of the lake.

The twelve ocean-derived algorithms selected for the comparison are the Aiken-C, Aiken-P, CalCOFI two-band linear, CalCOFI two-band cubic, CalCOFI three-band, Coastal, Morel-1, Morel-2, Morel-3, Morel-4, Oc2v4, and Oc4v4. All of these algorithms are based on various ratios of R_{rs} or L_{wn} measured in 20 nm wide optical bands centered at 443 nm, 490 nm, 510 nm, and 555 nm. Table 1 shows the mathematical form of each algorithm, with algorithms ordered based on the specific band ratios used. As shown in Fig. 2, these bands generally span the maximum and minimum absorption of visible radiation for phytoplankton, as measured based on diffuse spectral reflectance from a water sample collected from Lake Erie during July 2003 and filtered onto a Watman™ GF/F filter with an effective pore size of ~0.7 μm. The 443 nm band, occurring in the visible blue, is strongly absorbed by phytoplankton, while the 555 nm band, in the visible yellow-green, has stronger reflectance. Standard statistical techniques were used to evaluate the satellite-based chlorophyll concentration estimates. Least-square regression was applied to find the best linear relationship between the field observations and the satellite-based estimates. The correlation coefficient (r) and root mean square error (RMSE) were also calculated for each of the comparisons.

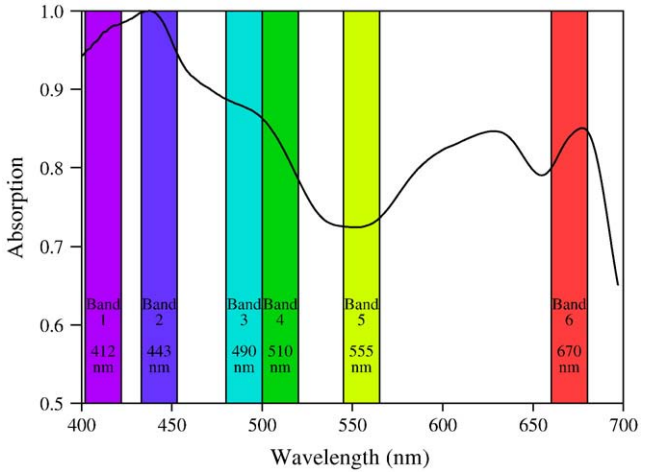

Fig. 2. Fractional absorption of visible and near-infrared radiation as measured for a GF/F-filtered Lake Erie water sample from the western Basin. The spectrum is a blank-corrected average of ten ensemble replicates using an Analytical Spectral Devices (ASD) Labspec Pro FR UV/VIS/nIR spectrometer (2 nm VIS resolution; 4–10 nm nIR resolution) equipped with an ASD High Intensity Contact Probe. Each individual ensemble replicate represents an integration of 200 individual spectra. Absorption values have been blank-corrected using an ensemble-averaged blank spectrum generated in the same fashion to remove the optical properties of the GF/F filter. SeaWiFS spectral bands at visible wavelengths are shown as shaded regions.

Results

Oceanic algorithms

When considered for the lake as a whole (Fig. 3), all of the oceanic algorithms had one or more undesirable features in statistical comparisons with the field data. Correlations between chlorophyll *a* concentrations measured from the field-collected samples and estimated using the satellite observations varied from 0.61 to 0.73. For nine of the twelve algorithms, the slope of the best fit line was less than 0.7 and the intercept of the best fit line was greater than 2.0 μg/L, with no algorithm producing a slope greater than 0.88 or an intercept less than 1.0 μg/L. Particularly problematic was estimation of low chlorophyll *a* concentrations, which tended to be overestimated by most algorithms. With the exception of the Aiken-C and Coastal algorithms, which produced the smallest dynamic ranges in the satellite estimates, chlorophyll concentration estimates from the ocean-derived algorithms were biased high at low chlorophyll concentrations. A second problem occurred at higher chlorophyll *a* concentrations (>5–8 μg/L), where about half of the algorithms underestimated chlorophyll concentration.

When the analysis was restricted to the western basin, correlations between the field and satellite chlorophyll estimates were lower than values obtained from the entire lake. Correlation coefficients calculated from only western basin data ranged from 0.53 to 0.63, and intercepts for the best linear fit ranged from to 1.69 to 5.30 μg/L, with nine algorithms producing intercepts greater than 3.0 μg/L. The slope of the best fit line varied significantly among the algorithms, with the lowest slope of 0.16 produced by the Coastal algorithm and the highest slope of 0.71 produced by the Morel-3 algorithm. If the western basin is eliminated from the analysis, the correlation coefficients and intercepts improve, but overly flat slopes are still obtained.

Sensitivity tests indicate that the misfits evident in Fig. 3 cannot be explained by the choice of the temporal collocation window or the data screening criteria. The average RMSE from the 12 ocean-derived algorithms was nearly identical (2.419 μg/L versus 2.421 μg/L) for comparisons restricted to same-day satellite and field sampling and for comparisons based on a broader temporal collocation window that also included samples within $\Delta t = \pm 1$ day. Somewhat better correlations ($r = 0.70$ versus $r = 0.61$) were actually obtained with the larger dataset available for the broader temporal window. When statistics from the 12 ocean-derived algorithms were compared for: (1) a dataset that eliminated collocated observations from days with greater than 20% of lake pixels masked and (2) a dataset that did not include this criterion, higher correlations were obtained for each of the 12 algorithms when the 20% lake-wide masking criteria was

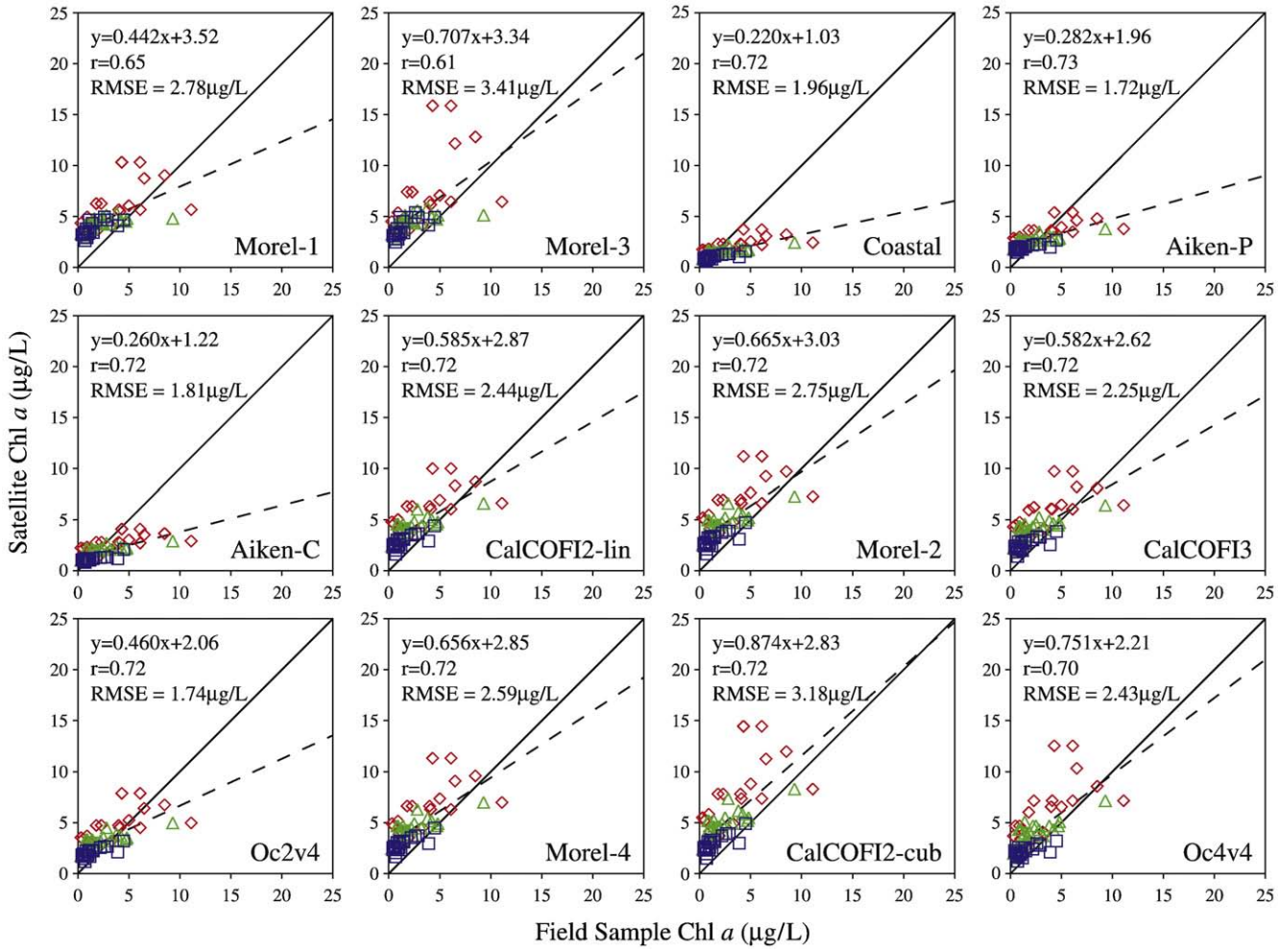

Fig. 3. Comparison of spatially and temporally collocated chlorophyll *a* concentrations measured from water samples with estimated concentrations from twelve ocean-derived algorithms applied to SeaWiFS observations (see Table 1). The equation of the best fit line through the data, the root mean squared error (RMSE), and the correlation coefficient, *r*, are provided for each comparison. Diamonds, triangles and squares depict observations from the western, central and eastern basins of Lake Erie, respectively. Algorithms are ordered by their mathematical form (see Table 1).

implemented, indicating that this criteria helped remove lower-quality observations. Sensitivity of the results to the choice of minimum distance to the closest masked pixel indicated that, for the 12 ocean-derived algorithms, average correlation coefficients were higher and the average RMSE values were lower for a 5 km proximity threshold as compared with implementation of no proximity threshold. Use of stricter screening was explored (i.e., a maximum of 10% lake-wide masking, a minimum of 10 km to the nearest masked pixel) but found to have relatively little impact on the statistics.

To aid in understanding the geographic variations in the quality of chlorophyll *a* estimates obtained within the various basins of the lake, parameters of the statistical comparisons calculated from the individual basins of the lake, as well as from all 68 collocated observations from entire lake, are presented in Fig. 4. Each panel of Fig. 4 displays one parameter of the statistical comparison, including the correlation coefficient (Fig. 4a), slope of the best fit line (Fig. 4b), intercept of the best fit line (Fig. 4c) and RMSE (Fig. 4d). In each of these panels, a perfect relationship between the field and satellite-based chlorophyll *a* concentrations (i.e., a correlation of 1.0, a best fit line with slope equal to 1.0 and an intercept equal to 0.0, and an RMSE of 0.0) is indicated by the horizontal dashed line. The range of variability obtained from among the twelve ocean-derived algorithms can be gauged from the shaded boxes in Fig. 4, which encompass the region between the 25th and 75th percentiles for each parameter, and from the thin vertical lines, which depict the range between the minimum and maximum values of each statistical parameter from the twelve ocean-derived algorithms.

Results from this comparison demonstrate a general improvement in three of the four statistical parameters as the region of interest moves from west to east. Exceptionally poor comparisons were obtained in the shallow western basin, where turbidity due to the large input of suspended sediment via rivers and the resuspension of this material may confound the biological lake color signal. Statistical comparisons were significantly better in the eastern basin of the lake, with strong improvements observed for the correlation coefficient, the intercept of the best fit line and the RMSE. In addition to variations of in-water properties, other potential sources of the observed variations include systematic differences in atmospheric or illumination conditions among the three basins.

The difference in typical chlorophyll *a* concentrations among the three basins was considered as a possible explanation for the variations evident in Fig. 4. If the observations for each basin are stratified into bins based on their field-measured chlorophyll *a* concentration (e.g., 0–2 µg/L, 2–4 µg/L, 4–6 µg/L), and the ratio of RMSE to median chlorophyll *a* concentration is computed from the data within each bin, the largest ratios occur in the western basin, with smaller values in the central basin, and smallest values in the eastern basin. (Note that this ratio could not be calculated for chlorophyll *a* concentrations between 4 and 6 µg/L in the eastern basin due to an insufficient number of observations). This indicates

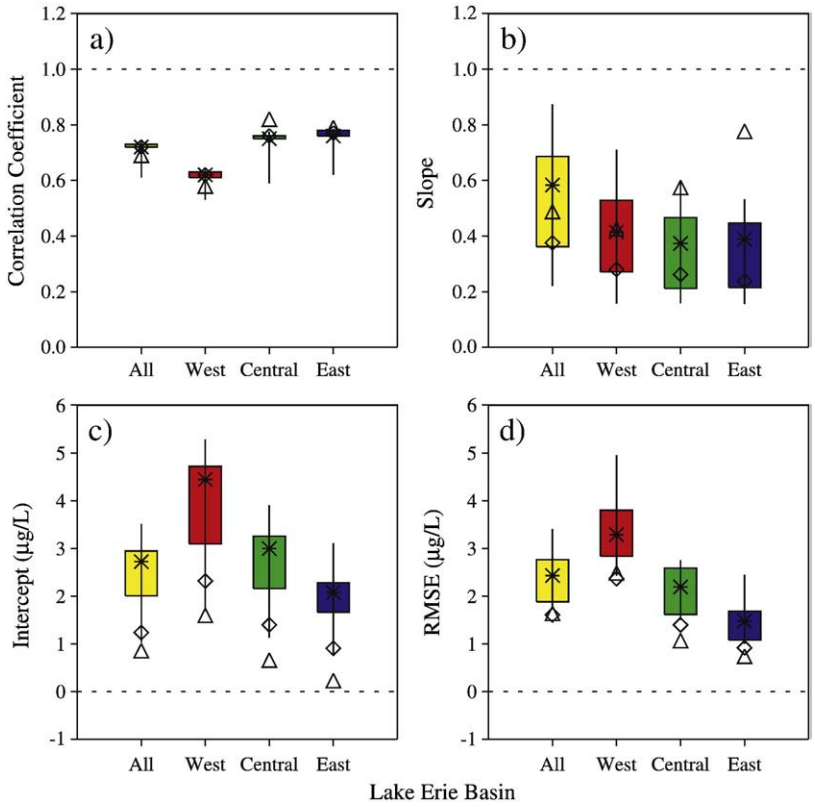

Fig. 4. Variations in statistical parameters calculated from comparisons of in-water chlorophyll *a* measurements with satellite-based estimates using various bio-optical algorithms. Parameters include (a) correlation coefficient, (b) slope of best fit line, (c) intercept of best fit line and (d) root mean squared difference between in-water measurements and satellite estimates. Values are shown for calculations from four regions of Lake Erie, including the combined western, central and eastern basins ("all") and each basin individually. For the 12 ocean-derived algorithms, the shaded rectangle encompasses the 25th through the 75th percentiles of each parameter, the thin vertical line shows the range between the minimum and maximum values and the asterisk indicates the median value. The diamonds show values obtained by applying the Darecki and Stramski (2004) regional Baltic Sea algorithm to the Lake Erie data, while the triangles show values obtained from the Lake Erie regional algorithms. The horizontal dashed line indicates the optimal value for each parameter.

that the large scatter observed in Fig. 3 for the western basin is not an artifact of the generally higher chlorophyll *a* concentrations found in this region. Even at low values of chlorophyll *a* concentration, the ocean-derived algorithms produce considerably more scatter in the western basin than in other regions of the lake, with scatter decreasing toward the east.

While several of the statistical parameters exhibited improvement from west to east, the slope of the best fit line was low for all 12 algorithms in all regions of the lake. Slopes greater than 0.5 were obtained for only two algorithms in the central basin (CalCOFI2-cub and Oc4v4) and two algorithms in the eastern basin (Morel-3 and CalCOFI2-cub). One result of this is that the dynamic range of chlorophyll *a* estimated from the satellite is significantly smaller than the dynamic range measured from the field samples. At low values of chlorophyll *a* concentration, only the Coastal and Aiken-C algorithms do not substantially underestimate the chlorophyll *a* concentration in the central and eastern basins. At larger chlorophyll *a* concentrations, many algorithms substantially underestimate these values.

A regional algorithm derived for Case 2 inland waters

Results from the analysis of the 12 oceanic algorithms thus indicate that, while correlations between measurements from field samples and satellite-based estimates improve from west to east, even in the eastern basin, the oceanic algorithms do not perform adequately. One approach to this dilemma is to use a regional algorithm that is tuned for the optical properties of inland water bodies that are more productive and more turbid than most regions of the ocean. One such possibility is an algorithm developed for the Baltic Sea based on an extensive set of in-water optical observations (Darecki and Stramski, 2004).

The Baltic Sea is a shallow and productive water body that is connected to the North Sea via the narrow Danish Straits. The atmosphere over the Baltic Sea is strongly influenced by terrestrial processes and the waters of the Baltic Sea can carry significant quantities of suspended sediment and CDOM. The predominance of Case 2 water in the Baltic Sea provided the motivation for Darecki and Stramski (2004) to explore the limitations of applying ocean-derived algorithms, which are generally tuned for Case 1 conditions, to the Baltic Sea environment, and then, to ultimately derive their own algorithm for this environment. While their algorithm reduced errors in satellite chlorophyll *a* retrievals, unresolved issues, particularly those involving the atmospheric correction, precluded Darecki and Stramski from recommending that the algorithm be used for chlorophyll *a* monitoring in the Baltic Sea region. This algorithm does however represent an attempt to obtain more valid satellite retrievals from optically complex waters.

The Darecki and Stramski Baltic Sea regional bio-optical algorithm (see Table 1) was developed for the MODIS wavebands. Here, we apply this algorithm to the Lake Erie dataset to explore whether using an algorithm derived specifically for a large inland body which includes Case 2 waters might produce better results than the oceanic algorithms described above. Values of L_{wn} at the 20 nm wide SeaWiFS bands centered on 490 nm and 555 nm are substituted for values of L_{wn} at the 10 nm wide MODIS bands centered at 488 nm and 551 nm, respectively. While this substitution will introduce an additional component of error, this error contribution is expected to be small

compared to other sources (e.g., inadequately corrected atmospheric effects), based on spectral properties of filtered Lake Erie water samples (Fig. 2) and based on the sensitivity of the SeaWiFS atmospheric correction to variations in the position of spectral bands (Wang, 1999).

The resulting satellite chlorophyll *a* estimates are plotted against the values of chlorophyll *a* measured from the water samples (Fig. 5). Like the oceanic algorithms, there is a clear improvement in the statistics of the comparison as the region of interest moves from the western to the central to the eastern basin of the lake. In all three basins however, the resulting comparisons suffer from problems similar to those observed for the oceanic algorithms, a result that was also obtained by Darecki and Stramski (2004) in their Baltic Sea analysis. In particular, correlations are too low, the intercept calculated for the best fit line is too high, and the slope of the best fit line is unacceptably low.

In Fig. 4, statistical parameters from the Baltic Sea algorithm are plotted as diamonds, allowing a more direct comparison between the performance of this algorithm and that of the twelve oceanic algorithms listed in Table 1. The correlation coefficient obtained for the Baltic Sea algorithm is comparable to those obtained from the oceanic algorithms (Fig. 4a). The slope of the best fit line for the Baltic Sea algorithms is less optimal than slopes obtained from most of the oceanic algorithms (Fig. 4b). Positive aspects of the comparison included the significantly lower intercept and lower RMSE values obtained with the Baltic Sea algorithm as compared with most of the oceanic algorithms (Figs. 4c, d).

Regional algorithms derived for Lake Erie

The approach of developing and applying a regional algorithm has been utilized in previous studies of chlorophyll *a* distributions within the Great Lakes (Budd and Warrington, 2004; Shuchman et al., 2006). For example, Li et al. (2004) derived regional algorithms and analyzed their performance in order to recommend approaches for improving satellite-based chlorophyll *a* retrievals for Lake Superior. To assess whether the approach of using a regional algorithm might improve chlorophyll *a* retrievals for Lake Erie, a set of regional algorithms was derived using the collocated Lake Erie field and satellite datasets. Linear, quadratic and cubic functional forms, similar to those used in the oceanic algorithms, were considered,

$$C = 10^{(a_0 + a_1 R)} \tag{1a}$$

$$C = 10^{(a_0 + a_1 R + a_2 R^2)} \tag{1b}$$

$$C = 10^{(a_0 + a_1 R + a_2 R^2 + a_3 R^3)} \tag{1c}$$

where R was represented as one of the following expressions:

$$R = \log(R_{rs443} / R_{rs555}) \tag{2a}$$

$$R = \log(R_{rs490} / R_{rs555}) \tag{2b}$$

$$R = \log(R_{rs510} / R_{rs555}) \tag{2c}$$

$$R = \log(\max[R_{rs443}, R_{rs490}, R_{rs510}] / R_{rs555}). \tag{2d}$$

The unknown coefficients, a_k, were determined based on least-squares regression using collocated data from the entire lake or using collocated data collected within each individual basin of the lake. Note that, because the algorithms have the form of power laws, they are not constrained to produce chlorophyll *a* estimates that cluster around a 1:1 line with respect to the field-based chlorophyll *a* measurements.

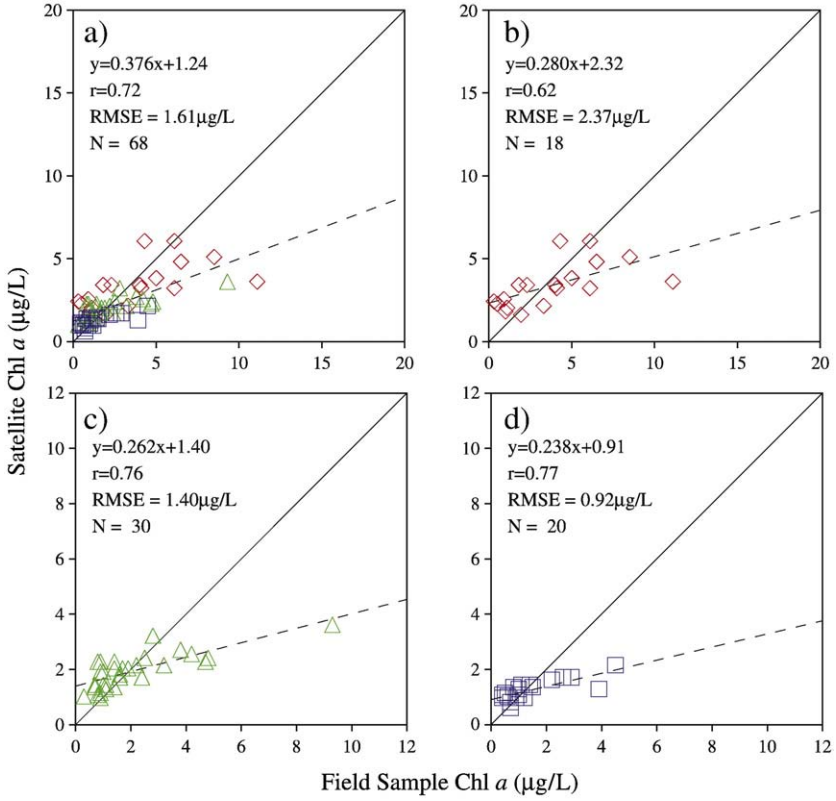

Fig. 5. Comparison of chlorophyll *a* measurements from Lake Erie water samples with chlorophyll *a* estimates obtained by applying the Darecki and Stramski (2004) Baltic Sea regional bio-optical algorithm to spatially and temporally collocated SeaWiFS observations. Each panel corresponds to a specific region of the lake: (a) entire lake, (b) western basin, (c) central basin, (d) eastern basin. The dashed line shows the best linear fit to the data, while the solid line shows the 1:1 relation. The equation for the best fit line, the correlation coefficient (r), the root mean squared error (RMSE), and the number of observations in the comparison (N) are shown for each region.

For example, the least-squares solution for the coefficients of the linear algorithm is derived by log-transforming Eq. (1a) and then using R as a dependent variable and $\log(C)$ as the independent variable.

Because of the small size of the collocated dataset, all of the collocated observations were used in determining algorithm coefficients, precluding the possibility of independently validating the algorithms using this dataset. These regional assessments therefore provide one "best case" indication of the results that might be obtained from regional algorithms of the mathematical form shown above. Such assessments are useful because if these "best case" results are inadequate, this clearly indicates that a different approach is needed. The nature of any inadequacies can then guide future approaches toward improved algorithm development. These approaches might include, for example, using alternative screening criteria, using alternate forms for atmospheric corrections, using more restrictive spatial and temporal collocation windows, using better corrections for the effects of unresolved CDOM and other CPAs, or using algorithms with different mathematical forms.

Algorithm performance was assessed based on the four statistical parameters shown in Fig. 4. The four linear algorithms (e.g., Eq. (1a) with Eqs. (2a)–(2d)) were first considered for the lake as a whole and for the eastern basin (the least optically complex of the lake regions). Within this group, algorithms based on R_{rs490}/R_{rs555} and R_{rs510}/R_{rs555} each performed best on two of the four metrics. With the addition of a quadratic term, algorithms based on R_{rs490}/R_{rs555} performed best on all four metrics in both regions. Adding the quadratic term significantly improved the slope and intercept of the best fit line in the eastern basin and produced a small improvement in these quantities for the lake as a whole. Adding a cubic term (Eq. (1c)) provided negligible improvement. In the western basin, all forms of algorithm performed poorly; for every algorithm, correlations were lower and the RMSE and the intercept of the best fit line were higher in the western basin than in the eastern basin. The slope of the best fit line was also much flatter in the western basin than the eastern basin for the majority of algorithm forms. In the central basin, algorithms based on R_{rs490}/R_{rs555} or R_{rs510}/R_{rs555} performed better on most metrics than those based on R_{rs443}/R_{rs555}, with quadratic algorithms producing more optimal slopes and intercepts than linear algorithms.

Fig. 6 compares chlorophyll a values measured from field samples with estimates obtained using quadratic Lake Erie regional algorithms derived with $R = \log(R_{rs490}/R_{rs555})$ for the lake as a whole (Fig. 6a) and for the three individual basins of the lake (Figs. 6b–d). The mathematical expressions for the whole lake, and western, central and eastern basin models are shown in the corresponding panels of Fig. 6. As noted above, quadratic algorithms based on the R_{rs490}/R_{rs555} band ratio outperformed other choices of algorithms in most regions of the lake as gauged from a variety of metrics. In Fig. 4, results from the Lake Erie regional algorithms are plotted as triangles.

For the western basin, the Lake Erie regional algorithm produced only a small improvement in the quality of chlorophyll a retrievals over those obtained from most of the ocean-derived algorithms or from the Baltic Sea algorithm. While the western basin regional algorithm produced a lower RMSE and intercept, the slope obtained with this algorithm was not distinctly different from those obtained with the oceanic algorithms and the correlation was slightly smaller than that obtained with most of the oceanic algorithms (see Fig. 4). Scatter in the satellite estimates of chlorophyll a is also problematic with this regional algorithm (see Fig. 6b).

In the central and eastern basins, regional algorithms produced improvements in all four statistical measures. Correlations and slopes obtained with the central and eastern basin regional algorithms are higher than those obtained with any of the other algorithms considered here, and intercepts and RMSE values are significantly lower (see Figs. 6c, d). At low chlorophyll a concentrations, most of the

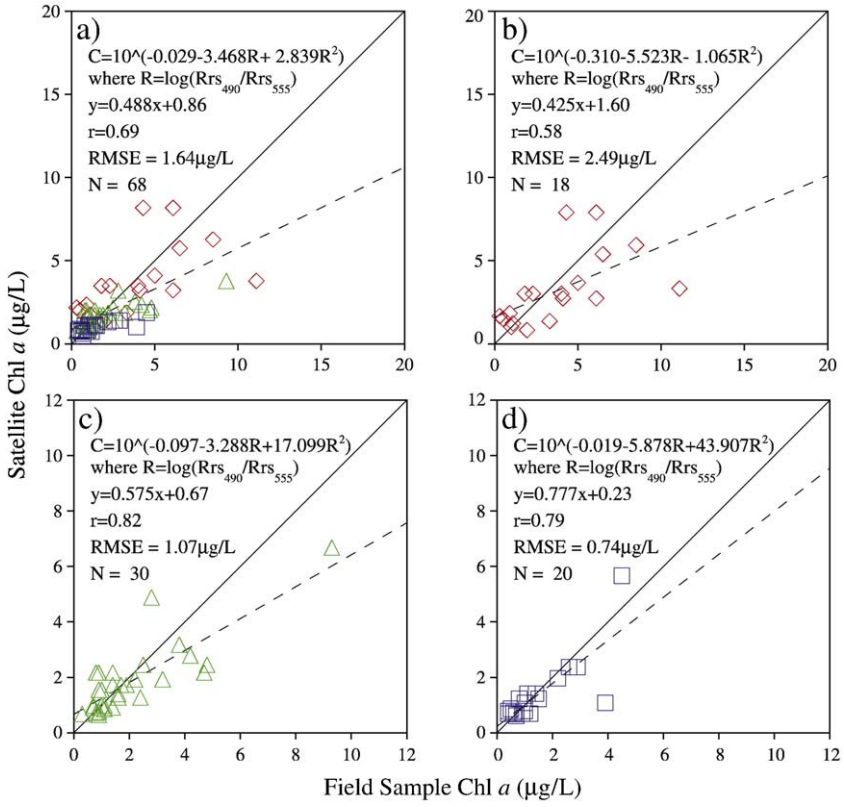

Fig. 6. Comparison of chlorophyll a measurements from Lake Erie water samples with chlorophyll a estimates obtained by applying regional algorithms developed for: (a) the entire lake, (b) the western basin, (c) the central basin, and (d) the eastern basin). The dashed line shows the best linear fit to the data, while the solid line shows the 1:1 relation. The equation for the satellite-based chlorophyll a concentration (C) is shown on each panel, along with the equation for the best fit line. The correlation coefficient (r), the root mean squared error (RMSE) and number of observations in the comparison (N) are shown for each region.

ocean-derived algorithms and the Baltic Sea algorithm overestimated concentrations. This problem was significantly less evident with the central basin regional algorithm (Fig. 6c) and not evident with the eastern basin regional algorithm (Fig. 6d). As a result, the best linear fit had a lower intercept and more optimal slope than those produced with other algorithms. Not unexpectedly, the significant improvement represented by the eastern and, possibly, central basin algorithms resulted in better performance for the regional algorithm derived using data from the entire lake (Fig. 6a).

Discussion and conclusions

Twelve ocean-derived algorithms for estimating chlorophyll *a* concentrations from SeaWiFS observations were evaluated for the three basins of Lake Erie. In the lake, biological and sedimentological materials within the water column can result in an optically complex and optically inhomogeneous environment. These particular algorithms were chosen as they have performed well over a wide range of chlorophyll *a* concentrations (O'Reilly et al., 1998, 2000). Of the twelve algorithms, none performs adequately in the lake as a whole or in any of the three sub-basins of the lake. In the western basin, the oceanic algorithms produce highly inaccurate estimates of the chlorophyll *a* concentration, and some algorithms fail to produce the dynamic range observed in the field dataset. In the eastern basin, scatter was less problematic, but at low chlorophyll *a* concentrations, the oceanic algorithms tend to produce estimates that are biased high. Results for the central basin are intermediate between those of the western and eastern basins.

Even under the most ideal conditions, a wide range of factors can contribute to differences between chlorophyll *a* concentrations measured from field-collected samples and estimates calculated using satellite-collected spectral data. These include differences in fluorescence measurements versus color-based estimates, effects of uncorrected atmospheric effects, differences due to inexact spatial and temporal collocation of paired field and satellite observations, variations in illumination in the satellite dataset, and errors introduced as a result of comparing chlorophyll *a* from a sample collected at a single depth and location with satellite observations which are representative of the optical depth of the water column, averaged over the pixel dimensions for the satellite sensor. In Lake Erie, these factors are further confounded by terrestrial influences on the atmosphere and by an inhomogeneous distribution with occasionally high loads of other CPAs within the water column (e.g., CDOM, suspended sediment, accessory pigments).

Because some aspects of the poor comparison between the in-water observations and satellite estimates may be due to the inland location of Lake Erie and the presence of Case 2 waters within it, the possibility of using a regional algorithm was explored. An algorithm derived by Darecki and Stramski (2004) for the Case 2, inland waters of the Baltic Sea produced slightly better comparisons with the field observations. This algorithm still suffered from many of the problems common to the oceanic algorithms, most notably high scatter at the western basin and systematic overestimation of low chlorophyll *a* concentrations.

Regional algorithms were then derived for the lake as a whole and for each individual basin of the lake. While the field dataset was not large enough to independently validate these algorithms, comparison of chlorophyll *a* measured from water samples and estimated from satellite observations provides a measure of the outlook for applying regionally developed algorithms to Lake Erie. The performance of these algorithms varied across the lake, with poorest results obtained for the western basin and the most optimal results obtained for the eastern basin. Of particular interest is the impact of the regional algorithms on the bias of the satellite estimates at low chlorophyll *a* concentrations. Systematic overestimates of low chlorophyll *a* concentrations obtained by applying oceanic algorithms to inland water have previously been attributed to CDOM in Lake Superior (Budd and Warrington, 2004; Li et al., 2004) and in the Baltic Sea (Darecki and Stramski, 2004). In Lake Erie, CDOM is known to covary with chlorophyll *a* (Twiss et al., 2006), and thus may contribute to a similar bias observed here at low chlorophyll *a* concentrations.

The very low scatter evident for the eastern basin regional algorithm indicates that unresolved atmospheric effects do not dominate the satellite signal in the eastern basin dataset used here. The influence of atmospheric contamination, as gauged from the percentage of masked pixels in the SeaWiFS dataset, does not vary substantially among the three basins, suggesting that, while some of the residual scatter observed with the regional algorithms may be due to unresolved atmospheric effects, it is likely that most of the residual scatter in the central and western basins is due to other factors. The western basin is known to have high loads of suspended sediment (Kemp et al., 1977; Marvin et al., 2007), and to have relatively high concentrations of algae with multiple accessory pigments (Ghadouani and Smith, 2005). These can confound the satellite signal, making it difficult to separate chlorophyll *a* from other CPAs. Other issues, such as differences in the spatio-temporal characteristics of the field and satellite samples, and small-scale variability (see, e.g., Vincent et al., 2004) may also contribute to the observed differences.

In most regions of Lake Erie, results from this study provide a positive outlook for the use of locally calibrated algorithms with mathematical forms similar to those used for the ocean. In the eastern basin, use of a regional algorithm greatly improves statistical measures of algorithm quality, indicating that an algorithm with a power-law form may be effective in this region of the lake. While there are some remaining issues in the central basin (particularly at higher chlorophyll concentrations), a regional approach using "ocean-like" algorithms also represents a significant improvement over direct use of oceanic algorithms there. In the western basin, the regionally calibrated algorithms considered here do not produce satisfactory results, and a different approach to algorithm development is needed.

In terms of the specific steps needed for algorithm improvement, a better understanding of the spectral characteristics of CPAs within the water is essential. These CPAs are a possible cause of the large scatter obtained for the western basin regional algorithm and the low slope of the best fit line in the central and western basins. While the dataset used in this study was extensive in terms of its geographic coverage, multiple years and multiple seasons of sampling, the number of valid field-satellite collocated pairs was small, precluding independent validation of the regional algorithms. Thus another important consideration for future field sampling is the need for a larger chlorophyll *a* field dataset for calibrating and independently validating satellite algorithms.

Acknowledgments

Support for Sarah Palm was provided by a Research Experience for Undergraduates grant by the National Science Foundation to the Kent State University Water Resources Research Institute (OCE-0139280 to R. Heath and L. Leff). Support for collection and analysis of water samples processed at Kent State University was provided by grant LEPF 98-09 from the Lake Erie Protection Fund and by grants R/ER-40-PD and R/ER-60 from Ohio Sea Grant. Support for processing of the SeaWiFS observations was provided by the Coastal Ocean Processes Program (OCE-9712872) and the Michigan Sea Grant College Program (project number R/ER-18), under federal grant NA16RG1145 from the National Sea Grant, National Oceanic and Atmospheric Administration, U.S. Department of Commerce, and funds from the State of Michigan. The authors thank the U.S. Environmental Protection Agency's Great Lakes National Program Office for providing water sample data through the Great Lakes Environmental Database (GLENDA). These data are available at http://www.epa.gov/glnpo/monitoring/data_proj/glenda/index.html.

References

Aiken, J.G., Moore, G.F., Trees, C.C., Hooker, S.B., Clark, D.K., 1995. The SeaWiFS CZCS-type pigment algorithm. In: Hooker, SB, Firestone, ER (Eds.), SeaWiFS technical report series, 29, pp. 1–34. NASA Tech. Memo. 104566.

Arar, E.J., Collins, G.B. 1997. Method 445.0 *in vitro* determination of chlorophyll *a* and pheophytin *a* in marine and freshwater algae by fluorescence. National Exposure Research Laboratory, Office of Research and Development, U.S. Environmental Protection Agency, 445.0-1, Revision 1.2.; p1–22.

Barbiero, R.P., Tuchman, M.L., 2001a. Results from the U.S. E.P.A.'s biological open water surveillance program of the Laurentian Great Lakes: I. Introduction and phytoplankton results. J. Great Lakes Res. 27, 134–154.

Barbiero, R.P., Tuchman, M.L., 2001b. Results from the U.S. E.P.A.'s open water surveillance programs of the Laurentian Great Lakes: II. Deep chlorophyll maximum. J. Great Lakes Res. 27, 155–166.

Beeton, A.M., 2001. Large freshwater lakes: present state, trends and future. Environ. Conserv. 29, 21–38.

Binding, C.E., Jerome, J.H., Bukata, R.P., Botty, W.G., 2007. Trends in water clarity of the lower Great Lakes from remotely sensed aquatic color. J. Great Lakes Res. 33, 828–841.

Budd, J.W., 2004. Large-scale transport phenomena in the Keweenaw Region of Lake Superior: the Ontonagon Plume and the Keweenaw Eddy. J. Great Lakes Res. 30 (Suppl. 1), 467–480.

Budd, J.W., Warrington, D.S., 2004. Satellite-based sediment and chlorophyll *a* estimates for Lake Superior. J. Great Lakes Res. 30 (Suppl. 1), 459–466.

Budd, J.W., Beeton, A.M., Stumpf, R.P., Culver, D.A., Kerfoot, W.C., 2001. Satellite observations of *Microcystis* blooms in western Lake Erie. Verh. Int. Ver. Theor. Angew Limnologie 27, 3787–3793.

Conroy, J.D., Quinlan, E.L., Kane, D.D., 2007. Culver DA. *Cylindrospermopsis* in Lake Erie: testing its association with other cyanobacterial genera and major limnological parameters. J. Great Lakes Res. 33, 519–535.

Darecki, M., Stramski, D., 2004. An evaluation of MODIS and SeaWiFS bio-optical algorithms in the Baltic Sea. Remote Sens. Environ. 89, 326–350.

Davis, J.C., 2002. Statistics and data analysis in geology, 3rd ed. New York, John Wiley and Sons.

Dusini, D.S., Foster, D.L., Shore, J.A., Merry, C., 2009. The effect of Lake Erie water level variations on sediment resuspension. J. Great Lakes Res. 35, 1–12.

Frost, P.C., Culver, D.A., 2001. Spatial and temporal variability of phytoplankton and zooplankton in Western Lake Erie. J. Freshw. Ecol. 16, 435–443.

Ghadouani, A., Smith, R.E., 2005. Phytoplankton distribution in Lake Erie as assessed by a new *in situ* spectrofluorometric technique. J. Great Lakes Res. 31 (Suppl. 1), 154–167.

Kemp, A.L.W., MacInnis, G.A., Harper, N.S., 1977. Sedimentation rates and a revised sediment budget for Lake Erie. J. Great Lakes Res. 3, 221–233.

Kerfoot, C.W., Budd, J.W., Green, S.A., Cotner, J.B., Biddanda, B.A., Schwab, D.J., Vanderploeg, H.A., 2008. Doughnut in the desert: late-winter production pulse in southern Lake Michigan. J. Great Lakes Res. 53, 589–604.

Li, H., Budd, J.W., Green, S.A., 2004. Evaluation and regional optimization of bio-optical algorithms for Central Lake Superior. J. Great Lakes Res. 30 (Suppl. 1), 443–458.

Makarewicz, J.C., 1993. Phytoplankton biomass and species composition in Lake Erie, 1970 to 1987. J. Great Lakes Res. 19, 258–274.

Makarewiczl, J.C., Lewis, T.W., Bertram, P., 1999. Phytoplankton composition and biomass in the offshore waters of Lake Erie: pre- and post-*Dreissena* introduction (1983–1993). J. Great Lakes Res. 25, 135–148.

Marvin, C.H., Charlton, M.N., Reiner, E.J., Kolic, T., MacPherson, K., Stern, G.A., Braekevelt, E., Estenik, J.F., Thiessen, L., Painter, S., 2002. Surficial sediment contamination in lakes Erie and Ontario: a comparative analysis. J. Great Lakes Res. 28, 437–450.

Marvin, C.H., Sverko, E., Charlton, M.N., Thiessen, P.A.L., Painter, S., 2004. Contaminants associated with suspended sediments in Lakes Erie and Ontario, 1997–2000. J. Great Lakes Res. 30, 277–286.

Marvin, C., Murray, C., Milne, J., Thiessen, L., Schachtschneider, J., Sverko, E., 2007. Metals associated with suspended sediments in Lakes Erie and Ontario, 2000–2002. Environ. Monit. Assess. 130, 149–161.

Mitchell, B.G., Kahru, M., 1988. Algorithms for SeaWiFS standard products developed with the CalCOFI bio-optical data set. In: Olfe, J (Ed.), California Cooperative Oceanic Fisheries Investigations reports, 39, pp. 133–147.

Mobley, C.D., Stramski, D., Bissett, W.P., Boss, E., 2004. Optical modeling of ocean waters: is the Case 1–Case 2 classification still useful? Oceanogr 17 (2), 60–67.

Morel, A., Prieur, L., 1977. Analysis of variations in ocean color. Limnol. Oceanogr. 22, 709–722.

National Geophysical Data Center, 1998. Bathymetry of Lake Erie and Lake Saint Clair CD-ROM. Product # G01363-CDR-A0001.

Ohio Lake Erie Commission. State of the Lake Report, 2004. Lake Erie quality index. Ohio Lake Erie Commission, Toledo, Ohio, p. 2004.

O'Reilly, J.E., Maritorena, S., Mitchell, B.G., Siegel, D.A., Carder, K.L., Garver, S.A., Kahru, M., McClain, C., 1998. Ocean color chlorophyll algorithms for SeaWiFS. J. Geophys. Res. 103, 24937–24953.

O'Reilly, J.E., Maritorena, S., Siegel, D.A., O'Brien, M.C., Toole, D., Mitchell, B.G., Kahru, M., Chavez, F.P., Strutton, M., Cota, G.F., Hooker, S.B., McClain, C.R., Carder, K.L., Müller-Karger, F., Harding, L., Magnuson, A., Phinney, D., Moore, G.F., Aiken, J., Arrigo, K.R., Letelier, R., Culver, M. 2000. Ocean color chlorophyll *a* algorithms for SeaWiFS, OC2 and OC4: version 4. SeaWiFS postlaunch technical report series. Vol. 11, Part 3, Ch. 2. NASA Goddard Space Flight Center, Greenbelt, MD. NASA-TM-2000-206892.

Ostrom, N.E., Carrick, H.J., Twiss, M.R., Piwinski, L., 2005. Evaluation of primary production in Lake Erie by multiple proxies. Oecologia 144, 115–124.

Painter, S., Marvin, C., Rosa, F., Reynoldson, T.B., Charlton, M.N., Fox, M., Lina Thiessen, P.A., Estenik, J.F., 2001. Sediment contamination in Lake Erie: A 25-year retrospective analysis. J. Great Lakes Res. 24, 434–448.

Shuchman, R., Korosov, A., Hatt, C., Pozdnyakov, D., Means, J., Meadows, G., 2006. Verification and application of a bio-optical algorithm for Lake Michigan using SeaWiFS: a 7-year inter- annual analysis. J. Great Lakes Res. 32, 258–279.

Smith, R.E.H., Hiriart-Baer, V.P., Higgins, S.N., Guildford, S.J., Charlton, M.N., 2005. Planktonic primary production in the offshore waters of Dreissenid-infested Lake Erie in 1997. J. Great Lakes Res. 31 (Suppl 2), 50–62.

Stumpf, R.P., Arnone, R.A., Gould, R.W., Martinolich, P., Ransibrahmanakul, V., Tester, P.A., Steward, R.G., Subramaniam, A., Culver, M., Pennock, J.R., 2000. SeaWiFS ocean color data for U.S. Southeast coastal waters. Proc. 6th int. conf. on remote sensing for marine and coastal environments, pp. 25–27.

Stumpf, R.P., Arnone, R.A., Gould Jr., R.W., Martinolich, P.M., Ransibrahmanakul, V., 2003. A partially coupled ocean-atmosphere model for retrieval of water-leaving radiance from SeaWiFS in coastal waters. In: Hooker, SB, Firestone, ER (Eds.), SeaWiFS postlaunch technical report series, vol. 22, algorithm updates for the fourth SeaWiFS data reprocessing, National Aeronautics and Space Administration Tech. Memo. 2003-206892, pp. 51–59.

Thuillier, G., Hersé, M., Simon, P.C., Labs, D., Mandel, H., Gillotay, D., Foujols, T., 2003. The solar spectral irradiance from 200 to 2400 nm as measured by the SOLSPEC spectrometer from the ATLAS 1-2-3 and EURECA missions. Sol. Phys. 214, 1–22.

Twiss, M.R., Page, D.I., Havens, S.M., Silsbe, G., Smith, R.E.H., 2006. Horizontal characterization of phytoplankton community composition and health. Lake Erie millennium network conference, Windsor, Ontario, Canada.

Vincent, R.K., Qin, X., McKay, R.M.L., Miner, J., Czajkowski, K., Savino, J., Bridgeman, T., 2004. Phycocyanin detection from LANDSAT TM data for mapping cyanobacterial blooms in Lake Erie. Remote Sens. Environ. 89, 382–392.

Wang, M., 1999. A sensitivity study of the SeaWiFS atmospheric correction algorithm: effects of spectral band variations. Remote Sens. Environ. 67, 348–359.